Accepted Manuscript

Open circuit potentiometry reports on internal redox states of cells in *G. Sulfurreducens* biofilms

Germán D. Schrott, P. Sebastián Bonanni, Juan Pablo Busalmen

PII: S0013-4686(19)30330-5

DOI: https://doi.org/10.1016/j.electacta.2019.02.078

Reference: EA 33669

To appear in: *Electrochimica Acta*

Received Date: 10 December 2018

Revised Date: 8 February 2019

Accepted Date: 17 February 2019

Please cite this article as: Germá.D. Schrott, P.Sebastiá. Bonanni, J.P. Busalmen, Open circuit potentiometry reports on internal redox states of cells in *G. Sulfurreducens* biofilms, *Electrochimica Acta* (2019), doi: https://doi.org/10.1016/j.electacta.2019.02.078.

Open circuit potentiometry reports on internal redox states of cells in *G. Sulfurreducens* biofilms.

Germán D. Schrott *, P. Sebastián Bonanni, Juan Pablo Busalmen.

División Ingeniería de Interfases y Bioprocesos, INTEMA-UNMDP-CONICET, Colón 10850, Mar del Plata, Argentina.

** Corresponding author: División Ingeniería de Interfases y Bioprocesos, INTEMA-UNMDP-CONICET, Colón 10850, Mar del Plata, Argentina. Tel.: +5402236260648. E-mail: germans@fi.mdp.edu.ar*

Keywords: *Geobacter sulfurreducens* • Biofilm • Bioelectrochemistry • Capacitor

Abstract

The outstanding capacity of *Geobacter sulfurreducens* cells to directly connect their inner electron transport chain to a polarized electrode have prompted the application of a wide arrange of electrochemical techniques to explore their metabolism and current production possibilities. In this work we use very basic electrochemical assays as open circuit potential, voltammetric and chronopotentiometric measurements to obtain fundamental information on bacterial electrochemical characteristics of importance to interpret bacterial functioning. Specifically, we obtained information on *G. sulfurreducens* biofilm capacity to store

charge in three major molecular reservoirs bridging the gap between NADH and the electrode, demonstrating, at the same time, the value of OCP measurements as a reporter of internal redox state of cells.

1. Introduction

When grown using a polarized electrode as the sole electron acceptor, *G. sulfurreducens* can produce thick conductive biofilms electrically connected to the electrode**[1]**. This amazing phenomena is structurally supported at the cell level by an arrangement of conductive molecules, which expands from the inner membrane all over the periplasmic space and across the outer membrane for transporting electrons to the extracellular environment**[2]**. Different molecules have been shown to be involved in extracellular electron transport, including c-type cytochromes, multi-copper proteins and conductive pili**[2–4]**, but c-type cytochromes are known to play a central role, not only in electron conduction but also in the respiration of a variety of electron acceptors, including iron compounds and electrodes**[5–9]**. More than 100 different genes for c-type cytochromes have been found in *G. sulfurreducens* that are expressed and translated under different environmental conditions**[10–12]**. Cytochromes are distributed along the internal and external membranes, the periplasmic space and the cell exterior. Among the most relevant cytochromes associated to electron conduction identified so far, ImcH**[13]** and CbcL**[14]** multi heme cytochromes are thought to connect the inner membrane to the periplasmic environment; the PpcA family, including 5 members of tri-heme periplasmic cytochromes, are the main electron conduit across the periplasmic

space to the outer membrane**[15]** and the periplasmic OmaB/OmaC and the outer membrane OmcB/OmcC cytochromes are a part of a porin complex involved in transferring electron from the periplasmic region to the cell exterior**[16]**, jointly with others recently informed redox active complexes that contain a periplasmic multiheme c-cytochrome, an integral outer membrane β-barrel and outer membrane redox lipoprotein**[17]**. Finally, external cytochromes as OmcS and OmcZ are most probably, the molecules responsible for making the electrical contact to solid external acceptors like metal oxides and electrodes**[5,8,18,19]**. Also cytochromes are thought to be involved in direct interspecies electron transfer (DIET)**[20]**, a process in which bacteria exchange electrons through conductive materials, redox molecules and conductive pili**[20,21]**.

Besides their unarguable role in electron conduction, cytochromes participate in charge storage**[22–27]**. In the eventual lack of electron acceptors, *Geobacter* cells sustain basal energy-dependent activities by transferring respiratory electrons to exocytoplasmatic cytochromes**[23]**, that become progressively reduced while accumulating charge in their heme groups. Interestingly, this phenomenon has also been observed in electricity producing biofilms when polarization is interrupted**[22]**. In this latter case, as accumulated charge can be recovered upon repolarization, modeling transient (discharge) current has been useful in estimating both the distribution of charge within biofilm compartments and the rate constants for electron transfer steps involved in electron conduction**[28,29]**.

In this work we use chronopotentiometry and cyclic voltammetry measurements to further investigate the charge storing process in *G. sulfurreducens* biofilms. Our results indicate the occurrence of at least three electron storing pools with different redox potentials, electrically connected to the electrode. The potential at which electrons are stored indicate that the selection of molecules where charge is stored depends on the pathway used by cells to release electrons from the cell interior which is indeed determined by the potential of the electron acceptor and the metabolic state of cells.

2. Experimental

2.1. Culture of microorganisms

Geobacter sulfurreducens strain DSM 12127 was anaerobically cultured at 30 ºC on a culture medium from that described elsewhere[30] and containing 30mM KCl, 100 mM $NaHCO_3$, 20 mM NaAc, 9.3 mM NH_4Cl, 2.5 mM NaH_2PO_4 anhydride, plus vitamins and trace minerals dissolved in distilled water. Sodium acetate 20 mM was used as the carbon source and the electron donor, while fumaric acid 40 mM was the electron acceptor[30].

2.2. Cell setup and biofilm generation.

All the experiments were performed in a custom made three electrode electrochemical cell using 0.4 cm in diameter graphite rods (XTG-15, Carbograf, Argentina) as the working electrode, a platinum wire as a counter electrode and an Ag/AgCl – 3 M NaCl (BASi RE-6) reference electrode. Working electrode surface

was treated as described in[22]. The exposed area of the working electrode was 2.76 cm^2. All potentials are here reported relative to SHE (i.e. 0.2V vs. Ag/AgCl). All system components (i.e. electrochemical reactor, medium reservoir, tubing, working and counter electrodes, magnetic bar, etc) were assembled prior autoclaving, in order to avoid steps of possible contamination. Just the reference electrode was added after autoclaving in a laminar flux after sterilization with alcohol at 70%. For biofilm growth 10 ml of an early stationary phase batch culture were inoculated into a biofilm reactor containing about 90 ml of deoxygenated culture medium lacking the electron acceptor and prepared as elsewhere[1]. When current generation reached 0.05 Am^{-2} a peristaltic pump was connected to continuously supply medium at a dilution rate of 0.02 h^{-1}. The reactor and all the liquid reservoirs in the continuous culture system were permanently flushed with a filtered gas mix of N_2:CO_2 to adjust the pH of the medium at 7.4 and to prevent the oxygen leakage to the system. The flush of gas on the liquid media also prevented possible interferences on the electrochemical measures due to the H_2 that may be produced on the counter electrode. Biofilms growth was followed by measuring the current output at a potential of 0.4 V (SHE). All the experiments were performed under permanent magnetic stirring and gas flushing into the reactors. At least three independent replicates were grown to obtain the reported results, *n* will be highlighted in the text when needed.

2.3. Electrochemical Assays.

All the experiments were performed using an Autolab PGSTAT101 potentiostat controlled by the Nova 1.6 dedicated software. For cyclic voltammetry the potential

was scanned between 0.6 and -0.5 V from an initial potential of 0.4 V scanning anodically. The scan rate was 0.01 $V.s^{-1}$ unless otherwise stated. Chronoamperometries during biofilms development and maintenance phases were performed at 0.4 V (SHE). OCP determination was performed acquiring potential values at 10 points per second. Chronopotentiometries were performed applying the selected current and collecting potential values at 10 points per second. In order to avoid biofilm damage, a final -0.45 V potential limit was settled. Between chronopotentiometries assays, the biofilms were polarized at 0.4 V in order to discharge the accumulated charge and set up a common starting point. Non-turnover electrochemical assays were performed after changing the cell electrolyte (i.e. growth media) for one lacking acetate under sterile and anoxic conditions.

3. Results and Discussion

3.1. Biofilm growth and charge accumulation

It has been previously shown that the open circuit potential (OCP) of an electrode functionalized with an active biofilm of *G. sulfurreducens* rapidly shifts toward negative values, due to the progressive reduction of bacterial electro-active molecules (e.g. c-type cytochromes) at the biofilm/electrode interface[22,28,31]. As the current that promotes that potential change is produced by the metabolic activity of the bacterial cells, we hypothesized that the measurement of the OCP has the potentiality to inform about the electrochemical potentials of involved electron storage sites. To further explore this phenomenon, in this work we

performed a series of OCP measurements, by opening the circuit at increasing times along biofilm development. Results obtained are presented in Fig.1 and Fig. S.1. A first OCP determination was performed shortly after current started to increase, marking the start of the exponential growth phase of the biofilm. As previously shown[22], at this stage biofilms producing a current of about 0.01 $A.m^{-2}$ drove the OCP of the working electrode to values of -0.197±0.01 V (n=2) (SHE) in about 120 min (Fig. 1, curve 1). Upon biofilm growth, OCP gradually achieved lower values and its evolution profile changed from the previously reported exponential decay, to a more complex response that included steps during which the electrode potential remained virtually constant. After about 60 hours of biofilm growth, when the biofilm was producing 0.025 $A.m^{-2}$ a first step on the OCP that expanded over 80 min was detected (Fig. 1, curve 2). During this time the potential remained at about -0.197±0.01 V (n=2) to latterly shift to more negative values. When the biofilm was producing 0.06 $A.m^{-2}$, the first step -0.207±0.005 V (n=4) was found to be much shorter (30 min) and was followed by a shift to a second stabilization potential of about -0.255±0.007 V (n=4) (Fig. 1, curve 3). Beyond 80 hours of biofilm growth, when current production was at 0.98 $A.m^{-2}$, that stabilization potential transformed into a new potential step that expanded over about 50 min and with a new stabilization value of -0.283+0.004 V (n=4) (Fig. 1, curve 4). At even higher currents (more than 2 $A.m^{-2}$), OCP curves did not show any step but a sharp drop to -0.318±0.018 V (n=4) within the first 10-20 min followed by the stabilization of the electrochemical potential at a final value of about -0.295 ±0.006 V (n=4) (Fig. 1, curves 5 and 6). It is important to highlight that polarization interruption did not produce any change in current development, which

evolved as in typical growth of a *G. sulfurreducens* biofilm (Fig. 1, inset), indicating that the experimental protocol did not disturb biofilm formation.

Steps shown in Fig. 1 are thought to be the result of the sequential reduction of different electro-active species (e.g. heme-groups) in electric contact to the electrode, by metabolic activity of biofilm cells. They can be interpreted as a typical constant current chronopotentiometry assay[32], in which the application of a negative current promotes the reduction of electro-active species at the electrode interface. In this assay, as redox molecules are reduced, the potential of the electrode equals that of the working redox couple and varies in time with the ratio of oxidized and reduced molecule forms. When all the molecules of the redox couple are reduced, the potential shifts towards more negative values, until another reduction process is reached, producing a step on the electrochemical potential.

In the case of the OCP measurement on biofilms, the electrons are not externally provided but produced by bacterial cells that continue transferring electrons to the external matrix even after interrupting electrode polarization. Electrons are stored in the reduced form of involved redox group(s)[23,31] and during each step the potential of the electrode equilibrates to the reduction potential of the working redox centers, until the oxidized form is exhausted. It is important to note that each step may not necessarily correspond to a single cytochrome type, as charge storage can occur in different redox molecules at the same potential, provided that they bear redox centers (i.e. hemes) with overlapping reduction potential windows and that they are electrically connected to each other and to the electrode.

While interpreting these results it is necessary to take into account that interruption of polarization causes a regulatory feedback on cells metabolism and respiration in

response to the sudden lack of the electron acceptor, thus influencing OCP changes presented above. A key element in this feedback is the NADH/NAD^+ redox couple which, acting as cofactor for regulatory enzymes, is reduced during catabolic reactions, to be latterly re-oxidized against complex I in the respiratory electron transport chain[33]. While the demand of NAD^+ during active metabolism is high, cytoplasmic concentration of the couple component is known to be relatively low and their redox turnover is in consequence very high[34]. Downstream, and by virtue of the molecular electric connection provided by the respiratory chain, the potential of the NADH/NAD^+ couple and that of the electron acceptor tend to equilibrate[22,34,35], but may differ depending on the balance between electron producing and consuming reactions kinetics. In the extreme situation of total lack of respiratory electron acceptors, as in the case of polarization interruption, electrons are no longer drained from the cells and progressively accumulate in electron carriers, ultimately causing a shift of the potential of the NADH/NAD^+ couple as NADH is accumulated[36]. Finally, the lack of NAD^+ determines the down regulation of electron producing catabolic reactions[33]. In this context, OCP values presented in Fig. 1 would, also, report the state of the cell internal redox balance and its change as a consequence of polarization interruption. Outside the cells, the redox gradient found in the extracellular matrix of biofilms as the distance to the electrode increases is known to limit respiration[37,38] and produce physiological stratification[1]. Recent measurements reported by Song *et. al.*[35] on the other hand demonstrate the dependence of the [NADH]/[NAD^+] ratio on the electrode potential in *G. sulfurreducens* cells, with cells exhibiting a higher ratio of reduced to oxidized NAD

as the potential decreases. According to this we propose that at every position within the biofilm the [NADH]/[NAD^+] ratio should equilibrate with the reduction state of the extracellular matrix, resulting in the observed physiological states[1]. Thereby, for using the partially reduced extracellular conductive matrix as electron acceptor cells located further away from the electrode should present a more negative internal potential. This gains importance when considering the influence of the electron acceptor potential on the pathway used by *Geobacter* bacteria to deliver electrons outside the cell[13,14,17,39,40]. Cells located in an oxidative environment in close contact to the electrode can produce electrons at high potential that, according to previous data[13], would reach the cell exterior through a high potential electron pathway initiated at the inner cell membrane by ImcH molecules. On the other hand, those cells located at the mostly reduced upper layers, may only release electrons at low potential and use a low potential pathway composed by CbcL molecules at the inner membrane[14].

It is important to note that due to respiratory constrains, as the biofilm grows and the redox gradient develops, the biofilm produces progressively more electrons, but the average potential at which those electrons are produced will decrease, resulting in an accelerated shift of the OCP value to the negative end as clearly observed in Fig. 1.

According to steps in Figure 1, S1 and the above discussion, at least two pools of heme groups are identified acting as electron storage sinks. They present increasing negative potentials of -0.207±0.005 V and -0.255±0.007 V vs. SHE and become evident at different stages of biofilm development, as the reducing power (i.e. the negative potential at with electrons are delivered) increases. Notably the

final OCP value of -0.295±0.006 V, is very close to the formal reduction potential of NADH (-0.32 V vs. SHE), the electron donor for the electron transport chain, supporting the idea of the OCP informing the redox state of the cell interior.

It is worth mentioning that when OCP determinations expanded for four hours, no further changes on the OCP patter were observed (Fig. S2), indicating that equilibrium on charge accumulation is reached after about two hours of polarization interruption.

Finally, it is interesting to highlight the occurrence of a minimum in the OCP curves on the mature biofilms, reaching potential values as low as -0.318±0.018 V (Fig. 1, S1, 2, S2 and S3) before stabilizing at a higher potential. We found two plausible explanations for this result. First, this behavior may indicate that hemes of cytochromes located near the electrode are reduced and to be latterly re-oxidized. An explanation to this phenomenon may be on possible differences in the electron transport rates inside the bacteria and through the extracellular matrix. Probably, upon polarization interruption, the electrons accumulated in the exocellular matrix would reach the electrode surface faster than those located inside the cells [28] due to a low rate of transport from the cell interior to the exocellular space. The accumulation of charge close to the electrode surface may yield a lower redox potential outside than inside the cells in that portion of the biofilm, producing the transport of a fraction of the exocellular charge to the cell interior. An alternative explanation may be the occurrence of pH gradients inside the biofilm during current production, with high acidification on the layers close to the electrode [41]. When electrode polarization is interrupted the production of protons by cell metabolism is suddenly ceased and then the pH in the biofilm slowly stabilizes with that of the

liquid media, producing changes in the pH on the biofilm layers close to the electrode and affecting the values of the OCP. This effect would be more evident for biofilms producing higher current densities due to existence of more pronounced pH gradients and higher biofilm thickness that lower the transport of protons out of the biofilm.

3.2. The role of physiology in the evolution of OCP curves

Further support to the previous interpretation comes from experiments done in the lack of electron donor (acetate). When the electron donor was removed from the system, the current density produced by *G. sulfurreducens* dropped down to a small fraction of its original value, in about 16 hours. OCP measurements were performed along this process on fully developed biofilms at increasing times after electron donor removal. As it can be seen in Fig. 2, (replicates shown in S3) the final OCP value in these measurements varied from -0.3±0.017 V (n= 3) before acetate depletion to about -0.27±0.015 V (n=3) after 24 hours of acetate removal. Notably the OCP curve profile at this time became very similar to that of early stage biofilms shown in Fig. 1, with a well-defined step at around -0.228±0.007 (n=3) V accompanied by a less evident one at about -0.123±0.02 (n=3) V vs. SHE. After 40 hours of starvation, OCP steps were more evident at all the three potentials (-0.246±0.015, -0.21±0.01 and -0.123+0.02 V, n=3). The fact that results obtained under non-turnover conditions where little current is produced are consistent with those obtained under turnover conditions indicates that H_2 that may

have been produced in the counter electrode during current production did not affect the OCP assays.

In the absence of the electron donor the metabolic capacity of cells to reduce NAD^+ sharply decreases, and they are no longer able to lower the internal redox potential. The electrical current is then remitted to the basal respiratory activity and, due to the small flow of electrons in the extracellular matrix, the extracellular redox potential equilibrates through all the biofilm as formerly shown[27,42]. Therefore, not only the number of electrons generated by the biofilm will decrease as the starvation extends in time, but also the cells capacity to deliver those electrons at more negative potentials. This combination progressively produces less negative OCP values and a prolongation on the time required to "fill" a charge reservoir, as seen on Fig. 2.

Interestingly, when acetate was provided again after two days of electron donor removal, OCP curves rapidly recovered previous patterns (Fig. S4), showing that biofilms remained viable. Changes like those presented in Fig. S4, produced in a relatively short period of time (30 minutes), can hardly be explained by changes in the composition of the molecular charge storing network. In place, these results further suggest that the OCP response is most likely related to the kinetics of electron production and the potentials at which biofilms can produce those electrons, which are in turn determined by the internal redox balance of cells. It is worth mentioning that after 60 hours without electron donor the OCP reached values of about -0.065±0.05 V (n=2), indicating that prolonged starvation led to a lack of cell-internal reducing power that impeded the reduction of heme groups with redox potentials below this limit.

3.3. Charge balance at electron reservoirs

In order to dig further in the charge storage process, we modified charge accumulation by imposing an electrical current to biofilms lacking an electron donor. During a classical chronopotentiometric assay, current is imposed to the electrode and the electrode potential is measured. In the present case, despite the lack of electron donor a small electrical current is produced by biofilm cells due to the remaining metabolic activity (Fig. 3 and S5). This internally produced current has to be also considered in order to correctly analyze the potential response on the chronopotenciometry assay.

Imposing an oxidative current of about 60% of the turnover current of the biofilm (i.e. restricting biofilm to respire the electrode at a higher rate) (Fig. 3, cyan curve), produced longer potential steps as compared to those observed at open circuit (Fig. 3, black line). This is interpreted as a consequence of electron drainage to the electrode, which increased the time required to fill electron reservoirs due to the lower net current flowing through the system. When reductive (negative) currents were applied, potential steps were shorter than those found in measurements at the OCP (Fig. 3, red and blue curves), indicating that the redox network was reduced faster due to the combined action of biological and electrochemical charging. The potential at which each step was observed did not vary with the imposed current, in clear agreement with the dependence of these values on the structure of involved molecules.

3.4. Comparison between OCP and cyclic voltammetry and localization of charge inside the biofilm

When a CV is performed under turnover conditions (with electron donor) on an electro-active biofilm, the redox process involved in the production of current cannot be identified; in place a typical sinusoidal signal is obtained in the response [43,44]. When the electron donor is removed from the media, oxidation and reduction of different redox elements in the biofilm can be observed. Voltammetric analysis of *G. sulfurreducens* in the absence of electron donor typically exhibit three main redox processes, with midpoint redox potentials of -0.28±0.008, -0.19±0.005 and -0.12±0.01 V vs. SHE (n = 4) (Fig. 4a) [27,45–47]. Interestingly, the midpoint potential of the processes observed on the CVs are very close to the values of the steps obtained in the OCP curves performed under the same conditions (Fig. 4a). Slight differences exist between the values of the CVs and those obtained on the OCP curves, because the determination of the redox potentials of cytochromes through CV depends on the reversibility of involved processes. Indeed, the overlap between the different oxidation-reduction processes and the interference of the small turnover current sometimes makes the identification of the peak's potential difficult, as in the case of the reductive counterpart of the process with the most negative redox potential (Fig. 4a).
By applying OCP to electro-active biofilms, redox potentials of involved species can be more accurately determined than by cyclic voltammetry. As mentioned before, if the OCP measurement is interpreted as a chronopotentiometry, the redox potential of the redox species connected with the electrode can be directly

determined by observing the values of the potential steps. Interestingly, this can be done on biofilms under turnover conditions, without the need of removing the electron donor from the media as in the case of the non-turnover CV.

When superposing OCP steps detected in measurements performed on acetate deprived biofilm with the redox active windows of *Geobacter* cytochromes and the reported reduction potential of their hemes (Fig. 4b, red curve) information about the possible charge storing cites can be obtained.

The three steps observed on the OCP measurement fall inside the redox window of periplasmic and extracellular cytochromes with each step expanding over the redox potential of groups of hemes present in different cytochromes (Fig. 4b). Moreover, the lower potential observed at -0.295±0.006 V in presence of electron donor (Fig 4b, black curve) falls on the lower bound of the redox window of the periplasmic cytochromes, that sets the lower limit for the potential at which charge can be accumulated inside and outside the cell. Interestingly, as shown in Fig 4b, the lower potential at which electrons are stored leaves a fraction of the redox range on exocellular cytochromes redox window that cannot be metabolically reduced.

We propose that the reduction of hemes of Ppc family, GSU1996 and MacA cytochromes, localized in the periplasm of *Geobacter* cells [11,12,15] and a fraction of the extracellular cytochromes, might be the origin of steps observed in the OCP curves.

4. Conclusions

OCP measurements may be a valuable tool for obtaining relevant information about the internal redox state of cells and improve the characterization of electro-active biofilms. We have applied this basic electrochemical technique for obtaining relevant information about charge accumulation in *G. sulfurreducens* biofilms. We were able to demonstrate that charge storage occurs in three main reservoirs, with average potentials close to those found in voltammetric signals that have been proposed to control electricity production. According to previously published data our results indicate that charge storing sites may be localized at both the periplasmic and extracellular space and that a fraction of the redox window of external cytochromes cannot be reduced by the cells.

OCP is a simple technique that can give important information about the process of charge storage in electro-active biofilms. For instance, OCP measurement on mutants lacking the genes coding for the inner membrane proteins that were proposed to set the redox potential of the extracellular electron transport process (ImcH and CbcL)[13,14], may produce valuable information on the way that these electron pathways operate.

Acknowledgements

The technical assistance of Juan Assarou and Hector Asencio are greatly appreciated. The financial support of iMETland project under contract #642190 and ANPCyT PICT project #0400/2015 are aknowledged.

References

[1] G.D. Schrott, M.V. Ordoñez, L. Robuschi, J.P. Busalmen, Physiological Stratification in Electricity-Producing Biofilms of Geobacter sulfurreducens, ChemSusChem. 7 (2013) 598–603. doi:10.1002/cssc.201300605.
[2] P.S. Bonanni, G.D. Schrott, J.P. Busalmen, A long way to the electrode: how do Geobacter cells transport their electrons?, Biochem Soc Trans. 40 (2012) 1274. doi:10.1042/BST20120046.
[3] N.S. Malvankar, D.R. Lovley, Microbial Nanowires: A New Paradigm for Biological Electron Transfer and Bioelectronics, ChemSusChem. 5 (2012) 1039–1046. doi:10.1002/cssc.201100733.
[4] M.V. Ordóñez, G.D. Schrott, D.A. Massazza, J.P. Busalmen, The relay network of Geobacter biofilms, Energy Environ. Sci. 9 (2016) 2677–2681. doi:10.1039/C6EE01699E.
[5] T. Mehta, M.V. Coppi, S.E. Childers, D.R. Lovley, Outer Membrane C-Type Cytochromes Required for Fe(III) and Mn(IV) Oxide Reduction in Geobacter sulfurreducens, Appl. Environ. Microbiol. 71 (2005) 8634. doi:10.1128/AEM.71.12.8634-8641.2005.
[6] D. Millo, F. Harnisch, S.A. Patil, H.K. Ly, U. Schröder, P. Hildebrandt, In Situ Spectroelectrochemical Investigation of Electrocatalytic Microbial Biofilms by Surface-Enhanced Resonance Raman Spectroscopy, Angewandte Chemie International Edition. 50 (2011) 2625–2627. doi:10.1002/anie.201006046.
[7] D.R. Lovley, Live wires: direct extracellular electron exchange for bioenergy and the bioremediation of energy-related contamination, Energy Environ. Sci. 4 (2011) 4896–4906. doi:10.1039/C1EE02229F.
[8] J.P. Busalmen, A. Esteve-Núñez, A. Berná, J.M. Feliu, C-Type Cytochromes Wire Electricity-Producing Bacteria to Electrodes, Angewandte Chemie International Edition. 47 (2008) 4874–4877. doi:10.1002/anie.200801310.
[9] M. Estevez-Canales, A. Kuzume, Z. Borjas, M. Füeg, D. Lovley, T. Wandlowski, A. Esteve-Núñez, A severe reduction in the cytochrome C content of Geobacter sulfurreducens eliminates its capacity for extracellular electron transfer, Environmental Microbiology Reports. 7 (2014) 219–226. doi:10.1111/1758-2229.12230.
[10] B.A. Methé, K.E. Nelson, J.A. Eisen, I.T. Paulsen, W. Nelson, J.F. Heidelberg, D. Wu, M. Wu, N. Ward, M.J. Beanan, R.J. Dodson, R. Madupu, L.M. Brinkac, S.C. Daugherty, R.T. DeBoy, A.S. Durkin, M. Gwinn, J.F. Kolonay, S.A.

Sullivan, D.H. Haft, J. Selengut, T.M. Davidsen, N. Zafar, O. White, B. Tran, C. Romero, H.A. Forberger, J. Weidman, H. Khouri, T.V. Feldblyum, T.R. Utterback, S.E. Van Aken, D.R. Lovley, C.M. Fraser, Genome of Geobacter sulfurreducens Metal Reduction in Subsurface Environments, Science. 302 (2003) 1967. doi:10.1126/science.1088727.
[11] Y.-H.R. Ding, K.K. Hixson, M.A. Aklujkar, M.S. Lipton, R.D. Smith, D.R. Lovley, T. Mester, Proteome of Geobacter sulfurreducens grown with Fe(III) oxide or Fe(III) citrate as the electron acceptor, Biochimica et Biophysica Acta (BBA) - Proteins and Proteomics. 1784 (2008) 1935–1941. doi:10.1016/j.bbapap.2008.06.011.
[12] Y.-H.R. Ding, K.K. Hixson, C.S. Giometti, A. Stanley, A. Esteve-Núñez, T. Khare, S.L. Tollaksen, W. Zhu, J.N. Adkins, M.S. Lipton, R.D. Smith, T. Mester, D.R. Lovley, The proteome of dissimilatory metal-reducing microorganism Geobacter sulfurreducens under various growth conditions, Biochimica et Biophysica Acta (BBA) - Proteins and Proteomics. 1764 (2006) 1198–1206. doi:10.1016/j.bbapap.2006.04.017.
[13] C.E. Levar, C.H. Chan, M.G. Mehta-Kolte, D.R. Bond, An Inner Membrane Cytochrome Required Only for Reduction of High Redox Potential Extracellular Electron Acceptors, MBio. 5 (2014) e02034-14. doi:10.1128/mBio.02034-14.
[14] L. Zacharoff, C.H. Chan, D.R. Bond, Reduction of low potential electron acceptors requires the CbcL inner membrane cytochrome of Geobacter sulfurreducens, Bioelectrochemistry. 107 (2016) 7–13. doi:10.1016/j.bioelechem.2015.08.003.
[15] T.C. Santos, M.A. Silva, L. Morgado, J.M. Dantas, C.A. Salgueiro, Diving into the redox properties of Geobacter sulfurreducens cytochromes: a model for extracellular electron transfer, Dalton Trans. 44 (2015) 9335–9344. doi:10.1039/C5DT00556F.
[16] Y. Liu, Z. Wang, J. Liu, C. Levar, M.J. Edwards, J.T. Babauta, D.W. Kennedy, Z. Shi, H. Beyenal, D.R. Bond, T.A. Clarke, J.N. Butt, D.J. Richardson, K.M. Rosso, J.M. Zachara, J.K. Fredrickson, L. Shi, A trans-outer membrane porin-cytochrome protein complex for extracellular electron transfer by Geobacter sulfurreducens PCA, Environmental Microbiology Reports. 6 (2014) 776–785. doi:10.1111/1758-2229.12204.
[17] C.H. Chan, C.E. Levar, F. Jiménez-Otero, D.R. Bond, Genome Scale Mutational Analysis of Geobacter sulfurreducens Reveals Distinct Molecular Mechanisms for Respiration and Sensing of Poised Electrodes versus Fe(III) Oxides, J. Bacteriol. 199 (2017) e00340-17. doi:10.1128/JB.00340-17.
[18] X. Qian, T. Mester, L. Morgado, T. Arakawa, M.L. Sharma, K. Inoue, C. Joseph, C.A. Salgueiro, M.J. Maroney, D.R. Lovley, Biochemical characterization of purified OmcS, a c-type cytochrome required for insoluble Fe(III) reduction in Geobacter sulfurreducens, Biochimica et Biophysica Acta (BBA) - Bioenergetics. 1807 (2011) 404–412. doi:10.1016/j.bbabio.2011.01.003.
[19] K. Inoue, X. Qian, L. Morgado, B.-C. Kim, T. Mester, M. Izallalen, C.A. Salgueiro, D.R. Lovley, Purification and Characterization of OmcZ, an Outer-Surface, Octaheme C-Type Cytochrome Essential for Optimal Current Production by Geobacter sulfurreducens, Appl. Environ. Microbiol. 76 (2010) 3999. doi:10.1128/AEM.00027-10.

[20] D.R. Lovley, Syntrophy Goes Electric: Direct Interspecies Electron Transfer, Annu. Rev. Microbiol. 71 (2017) 643–664. doi:10.1146/annurev-micro-030117-020420.
[21] F. Liu, A.-E. Rotaru, P.M. Shrestha, N.S. Malvankar, K.P. Nevin, D.R. Lovley, Promoting direct interspecies electron transfer with activated carbon, Energy Environ. Sci. 5 (2012) 8982–8989. doi:10.1039/C2EE22459C.
[22] G.D. Schrott, P.S. Bonanni, L. Robuschi, A. Esteve-Nuñez, J.P. Busalmen, Electrochemical insight into the mechanism of electron transport in biofilms of Geobacter sulfurreducens, Electrochimica Acta. 56 (2011) 10791–10795. doi:10.1016/j.electacta.2011.07.001.
[23] A. Esteve-Núñez, J. Sosnik, P. Visconti, D.R. Lovley, Fluorescent properties of c-type cytochromes reveal their potential role as an extracytoplasmic electron sink in Geobacter sulfurreducens, Environmental Microbiology. 10 (2007) 497–505. doi:10.1111/j.1462-2920.2007.01470.x.
[24] D.R. LOVLEY, Extracellular electron transfer: wires, capacitors, iron lungs, and more, Geobiology. 6 (2008) 225–231. doi:10.1111/j.1472-4669.2008.00148.x.
[25] A. Jain, G. Gazzola, A. Panzera, M. Zanoni, E. Marsili, Visible spectroelectrochemical characterization of Geobacter sulfurreducens biofilms on optically transparent indium tin oxide electrode, Electrochimica Acta. 56 (2011) 10776–10785. doi:10.1016/j.electacta.2011.02.073.
[26] Y. Liu, H. Kim, R.R. Franklin, D.R. Bond, Linking Spectral and Electrochemical Analysis to Monitor c-type Cytochrome Redox Status in Living Geobacter sulfurreducens Biofilms, ChemPhysChem. 12 (2011) 2235–2241. doi:10.1002/cphc.201100246.
[27] Y. Liu, D.R. Bond, Long-Distance Electron Transfer by G. sulfurreducens Biofilms Results in Accumulation of Reduced c-Type Cytochromes, ChemSusChem. 5 (2012) 1047–1053. doi:10.1002/cssc.201100734.
[28] P.S. Bonanni, G.D. Schrott, L. Robuschi, J.P. Busalmen, Charge accumulation and electron transfer kinetics in Geobacter sulfurreducens biofilms, Energy Environ. Sci. 5 (2012) 6188–6195. doi:10.1039/C2EE02672D.
[29] B. Virdis, D. Millo, B.C. Donose, Y. Lu, D.J. Batstone, J.O. Krömer, Analysis of electron transfer dynamics in mixed community electroactive microbial biofilms, RSC Adv. 6 (2016) 3650–3660. doi:10.1039/C5RA15676A.
[30] A. Esteve-Núñez, M. Rothermich, M. Sharma, D. Lovley, Growth of Geobacter sulfurreducens under nutrient-limiting conditions in continuous culture, Environmental Microbiology. 7 (2005) 641–648. doi:10.1111/j.1462-2920.2005.00731.x.
[31] N.S. Malvankar, T. Mester, M.T. Tuominen, D.R. Lovley, Supercapacitors Based on c-Type Cytochromes Using Conductive Nanostructured Networks of Living Bacteria, ChemPhysChem. 13 (2012) 463–468. doi:10.1002/cphc.201100865.
[32] A. J. Bard, L. R. Faulkner, Electrochemical Methods: Fundamentals and Applications, John Wiley & Sons, 2001.
[33] D. White, The Physiology and Biochemistry of Prokaryotes, Oxford University Press, New York, 1995.
[34] M.R. de Graef, S. Alexeeva, J.L. Snoep, M.J. Teixeira de Mattos, The Steady-State Internal Redox State (NADH/NAD) Reflects the External Redox State

and Is Correlated with Catabolic Adaptation inEscherichia coli, J. Bacteriol. 181 (1999) 2351.
[35] J. Song, D. Sasaki, K. Sasaki, S. Kato, A. Kondo, K. Hashimoto, S. Nakanishi, Comprehensive metabolomic analyses of anode-respiring Geobacter sulfurreducens cells: The impact of anode-respiration activity on intracellular metabolite levels, Process Biochemistry. 51 (2016) 34–38. doi:10.1016/j.procbio.2015.11.012.
[36] Logan Bruce E, Microbial Fuel Cells, John Wiley And Sons. Inc, Hoboken, 2008.
[37] P.S. Bonanni, D.F. Bradley, G.D. Schrott, J.P. Busalmen, Limitations for Current Production in Geobacter sulfurreducens Biofilms, ChemSusChem. 6 (2013) 711–720. doi:10.1002/cssc.201200671.
[38] L. Robuschi, J.P. Tomba, G.D. Schrott, P.S. Bonanni, P.M. Desimone, J.P. Busalmen, Spectroscopic Slicing to Reveal Internal Redox Gradients in Electricity-Producing Biofilms, Angewandte Chemie International Edition. 52 (2012) 925–928. doi:10.1002/anie.201205440.
[39] L. Peng, X.-T. Zhang, J. Yin, S.-Y. Xu, Y. Zhang, D.-T. Xie, Z.-L. Li, Geobacter sulfurreducens adapts to low electrode potential for extracellular electron transfer, Electrochimica Acta. 191 (2016) 743–749. doi:10.1016/j.electacta.2016.01.033.
[40] C.E. Levar, C.L. Hoffman, A.J. Dunshee, B.M. Toner, D.R. Bond, Redox potential as a master variable controlling pathways of metal reduction by Geobacter sulfurreducens, The Isme Journal. 11 (2017) 741.
[41] C.I. Torres, A. Kato Marcus, B.E. Rittmann, Proton transport inside the biofilm limits electrical current generation by anode-respiring bacteria, Biotechnology and Bioengineering. 100 (2008) 872–881. doi:10.1002/bit.21821.
[42] Robuschi L, Tomba JP, Busalmen JP, Proving Geobacter biofilm connectivity with confocal Raman microscopy, J. Electroanal. Chem. 793 (2017) 99–103. doi:10.1016/j.jelechem.2016.11.005.
[43] K. Fricke, F. Harnisch, U. Schröder, On the use of cyclic voltammetry for the study of anodic electron transfer in microbial fuel cells, Energy Environ. Sci. 1 (2008) 144–147. doi:10.1039/B802363H.
[44] E. Marsili, J. Sun, D.R. Bond, Voltammetry and Growth Physiology of Geobacter sulfurreducens Biofilms as a Function of Growth Stage and Imposed Electrode Potential, Electroanalysis. 22 (2010) 865–874. doi:10.1002/elan.200800007.
[45] N.S. Malvankar, M.T. Tuominen, D.R. Lovley, Comment on “On electrical conductivity of microbial nanowires and biofilms” by S. M. Strycharz-Glaven, R. M. Snider, A. Guiseppi-Elie and L. M. Tender, Energy Environ. Sci., 2011, 4, 4366, Energy Environ. Sci. 5 (2012) 6247–6249. doi:10.1039/C2EE02613A.
[46] K.P. Katuri, P. Kavanagh, S. Rengaraj, D. Leech, Geobacter sulfurreducens biofilms developed under different growth conditions on glassy carbon electrodes: insights using cyclic voltammetry, Chem. Commun. 46 (2010) 4758–4760. doi:10.1039/C003342A.
[47] K. Fricke, F. Harnisch, U. Schröder, On the use of cyclic voltammetry for the study of anodic electron transfer in microbial fuel cells, Energy Environ. Sci. 1 (2008) 144–147. doi:10.1039/B802363H.

Fig. 1. Open circuit potential measurement on growing *G. sulfurreducens* biofilms. *Geobacter* biofilms were grown in 3-electrodes electrochemical cells, using AcNa 20mM as electron donor and carbon source and a polarized (0.4 V vs. SHE) graphite rod electrode as unique electron acceptor. At different times along biofilm development, polarization was interrupted and the OCP was measured. Inset: example of current density curve along biofilm development interrupted to perform OCP determinations. Numbers indicate the times at which OCP measurements were performed. Independent biofilms replicates are provided in Fig. S1.

Fig. 2. OCP measurement in the lack of electron donor. The figure shows typical behavior of OCP measurement performed on mature *G. sulfurreducens* biofilms at increasing times since electron donor deprivation (i.e. growth media was replaced by one lacking acetate in sterile and anaerobic conditions). When the medium was changed, a little medium with acetate was left in the electrochemical cell in order to leave minimum electron donor availability and allow it to decay. Independent biofilms replicates are provided in Fig. S3.

Fig. 3: Potentiostatically control biofilm charging. A mature *G. sulfurreducens* biofilm without electron donor on the medium was left at open circuit and the potential was measured (black line). Later, chronopotentiometry assays with fixed current were performed. **Cyan**: oxidative current density of 0.038 Am^{-2} was applied to the electrode and the potential registered. **Red** and **Blue**: reductive current densities of -0.051 and -0.026 Am^{-2} were applied, respectively. Between each chronopotentiometry assay, the biofilm was polarized at 0.4 V (SHE) for 30 minutes, to discharge the cytochromes and set a standard starting point. Independent biofilms replicates are provided in Fig. S5.

Fig. 4: Relationship between non-turn over cyclic voltammetry and OCP determination. A) Midpoint potentials (red discontinue lines, n=4) of the three redox process observed in non-turnover voltammetry (inset) are superimposed to OCP curves. Black and blue curves correspond to typical OCP behavior for acetate lacking biofilm at increasing times since acetate removal, respectively. Grey line corresponds to OCP measurement of a fully developed biofilm in presence of electron donor. B) Schematic of electron storage process. NADH dehydrogenase transfer electrons to the menaquinone (MQ) pool, ImcH and CbcL quinone oxidase complex transfer electrons to periplasmatic cytochromes. Upon polarization interruption electrons travel to exocellular cytochromes, where charge start to accumulate on higher potentials hemes. Then, electrons reduce up stream hemes,

following a potential gradient. Rectangular boxes represent known redox active windows of internal and exocellular cytochromes at pH 7. Horizontal blue lines correspond to the reduction potential of the hemes for which data is available (taken from Santos et. al. 2015) [15]. Horizontal doted black lines represent the midpoint potential steps found the OCP assays. Red curve: OCP measurement of a fully developed biofilm under acetate depletion conditions. Black curve: OCP measurement of the same biofilm under turnover conditions.

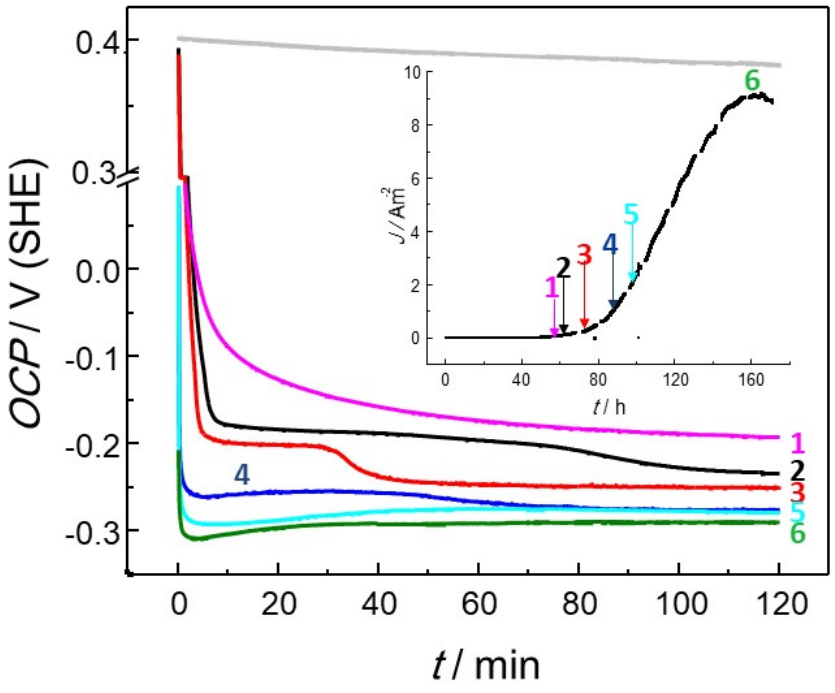
0.4
0.3
0.0
-0.1
-0.2
-0.3
OCP / V (SHE)
0
20
40
60
80
100
120
t / min
1
2
3
4
5
6
10
8
6
4
2
0
J / Am-2
0
40
80
120
160
t / h

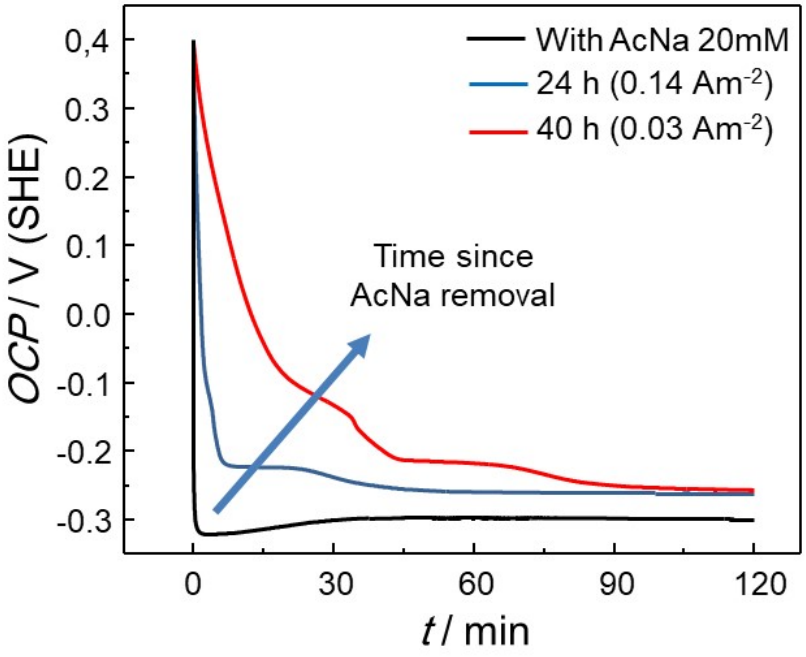
With AcNa 20mM
24 h (0.14 Am-2)
40 h (0.03 Am-2)
Time since
AcNa removal
OCP / V (SHE)
0,4
0.3
0.2
0.1
0.0
-0.1
-0.2
-0.3
0
30
60
90
120
t / min

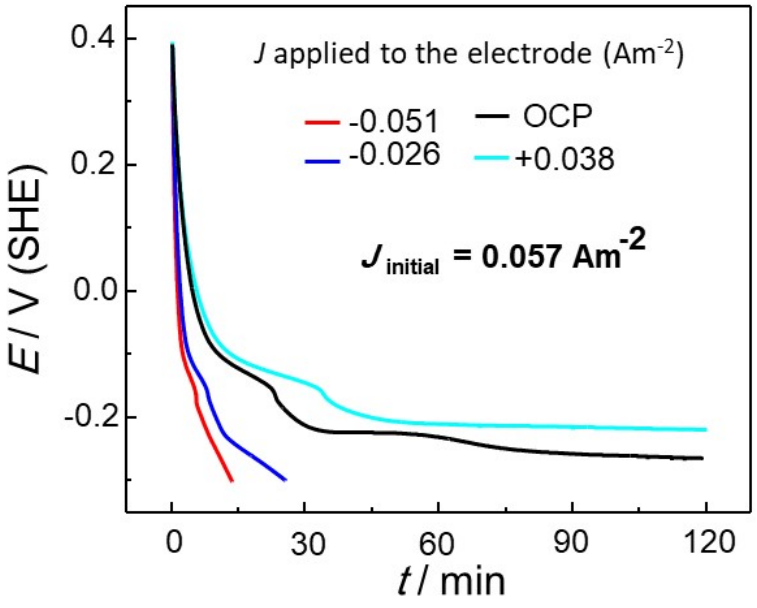
J applied to the electrode (Am-2)
-0.051
-0.026
OCP
+0.038
J initial = 0.057 Am-2
E / V (SHE)
t / min
0.4
0.2
0.0
-0.2
0
30
60
90
120

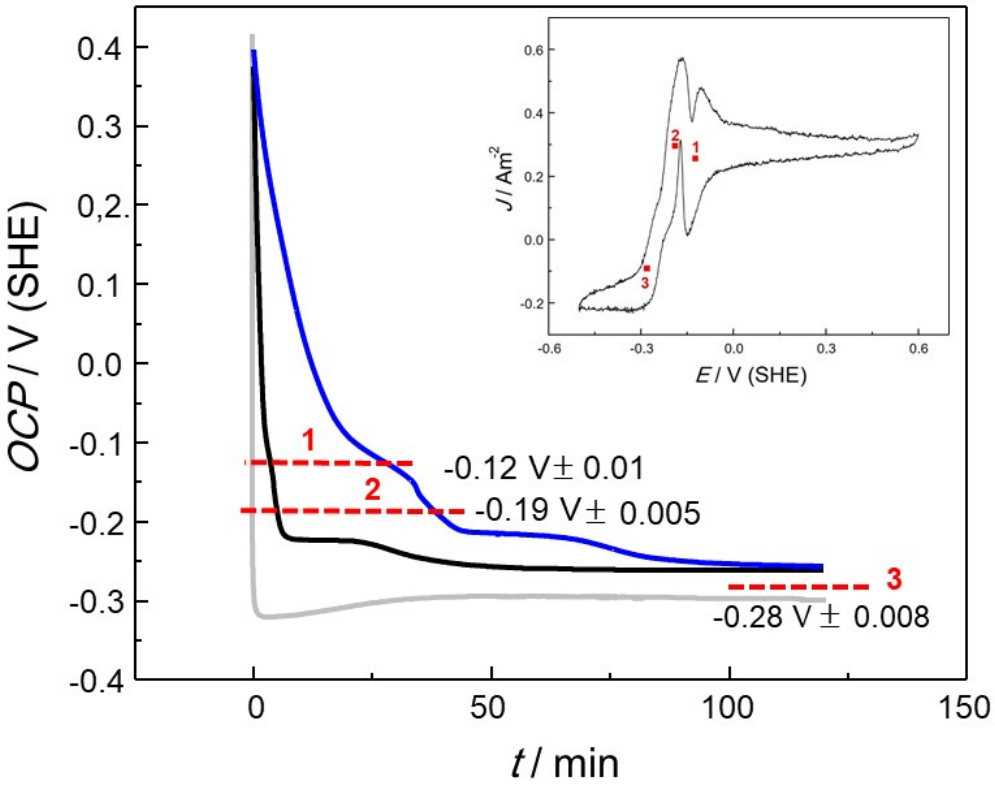
OCP / V (SHE)
t / min
0.4
0.3
0,2.
0.1
0.0
-0.1
-0.2
-0.3
-0.4
0
50
100
150
1
2
3
-0.12 V± 0.01
-0.19 V± 0.005
-0.28 V ± 0.008
J / Am-2
E / V (SHE)
0.6
0.4
0.2
0.0
-0.2
-0.6
-0.3
0.0
0.3
0.6

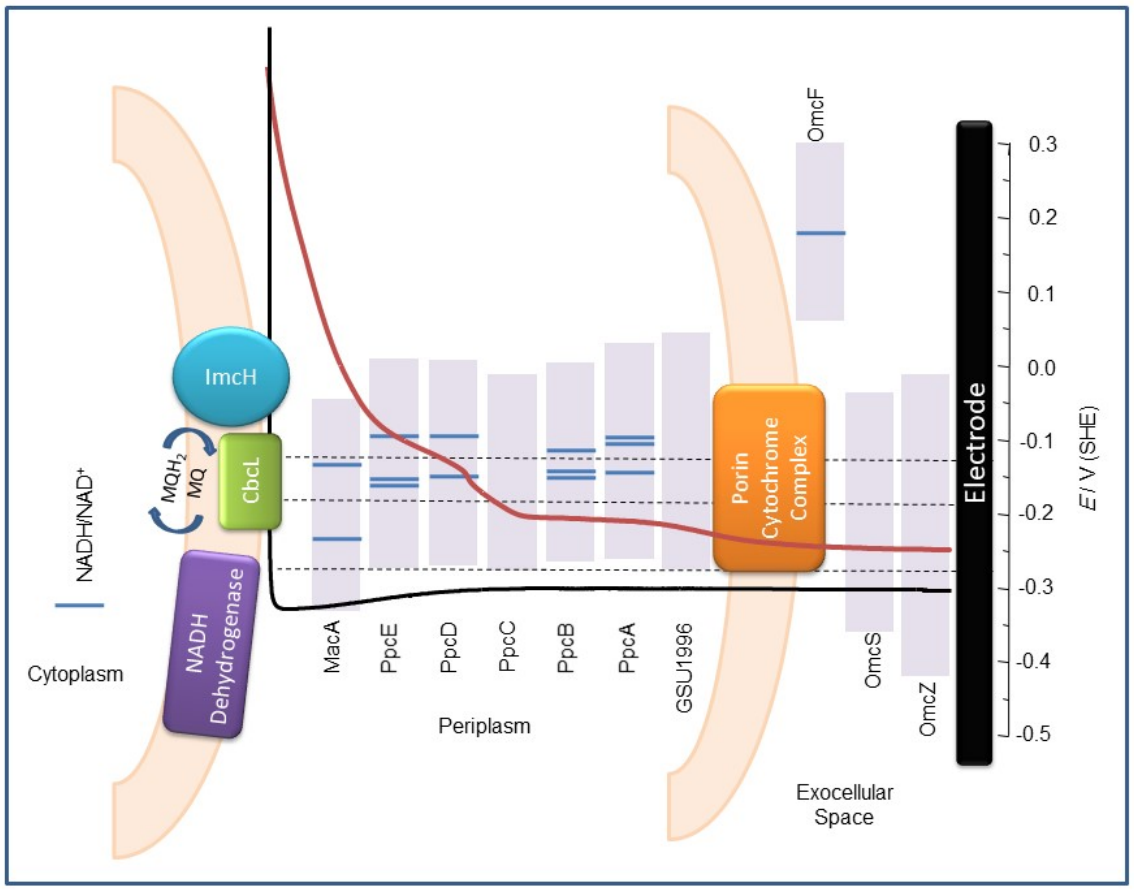
ImcH
CbcL
MQH_2
MQ
NADH/NAD+
NADH Dehydrogenase
Cytoplasm
MacA
PpcE
PpcD
PpcC
PpcB
PpcA
GSU1996
Periplasm
Porin Cytochrome Complex
OmcF
OmcS
OmcZ
Exocellular Space
Electrode
0.3
0.2
0.1
0.0
-0.1
-0.2
-0.3
-0.4
-0.5
E / V (SHE)